The Structure of Human Parathyroid Hormone from a Study of Fragments in Solution Using ^{1}H NMR Spectroscopy and Its Biological Implications

Victor Wray,*,‡ Torsten Federau,‡ Wolfram Gronwald,‡ Hubert Mayer,§ Dietmar Schomburg,‡ Werner Tegge,‖ and Edgar Wingender§

Abteilung für Molekulare Strukturforschung, Abteilung für Genetik, and Arbeitsgruppe für Peptid Synthese, GBF—Gesellschaft für Biotechnologische Forschung, Braunschweig, FRG

Received September 8, 1993; Revised Manuscript Received December 1, 1993®

ABSTRACT: In order to gain insight into the structure of human parathyroid hormone (hPTH), four fragments [hPTH(1–34), hPTH(18–48), hPTH(28–48), and hPTH(53–84)], which cover all regions of the intact hormone, have been investigated by CD and NMR spectroscopy in combination with distance geometry, and restrained molecular dynamics and energy minimization calculations, under a variety of solution conditions. Significantly, all fragments showed little propensity to form stable structures in aqueous solution alone, and it was only on the addition of trifluoroethanol (TFE) that defined structural features were observed. In an extension of earlier work [Klaus et al. (1991) *Biochemistry 30,* 6936–6942], hPTH(1–34) in 70% trifluoroethanol (TFE) showed two helices that were longer than in 10% TFE, but essentially showed the same characteristics. Although overlap in the ^{1}H NMR spectra prevented the determination of quantitative NOE data for residues 26–30, the combination of the α-proton chemical shift data and quantitative NOE data indicated the helices extend from residues 3 to 13 and 15 to 29. No evidence was found for interaction of the two helical regions. The nature and extent of this second helix in the intact hormone were better defined from the data for hPTH(18–48). Under limiting solution conditions, where the fragment assumed its maximum helical content, a well-defined helix was observed between residues 21 and 38 with a possible discontinuity between Leu-28 and Gln-29. There was little evidence of any form of secondary structure between Gly-38 and the terminus of this fragment, Ser-48. In keeping with this result, the shorter fragment, hPTH(28–48), showed little evidence of stable secondary structure on addition of TFE. From the α-proton chemical shifts residues 23–27 appeared to sustain helical structure more readily than the rest of molecule under all solution regimes in both hPTH(1–34) and hPTH(18–48). In contrast to the other two longer fragments hPTH(53–84) showed little propensity for helical secondary structure even at the highest TFE concentrations. However, there was evidence that the molecule did adopt a defined three-dimensional structure. Various long-range NOE's were observed in 10% TFE that allowed the calculation of an open teriary structure consisting of an initial series of turns surrounded by a loop structure of several loose turns. Using these results, a model of the structural characteristics of the intact hormone, under conditions that simulate the membrane-like environment, was constructed and compared schematically with the large amount of *in vitro* and *in vivo* activity data that exists in the literature for the intact hormone and its fragments. The correlation between various structural features and activity is pointed out, and the apparent importance of the α-helical regions, in the N-terminal half of the molecule, for binding to the membrane-bound G-protein-coupled receptors is discussed.

Considerable attention has been focused on the 84 amino acid peptide hormone, human parathyroid hormone (hPTH),[1] as its main function is to regulate the calcium homeostasis in the serum through a cAMP-dependent mechanism. In this respect the first 34 N-terminal residues in the sequence show *in vitro* and *in vivo* activities comparable with those of the intact hormone; hence, the majority of structural studies have concentrated on this fragment. Recently, however, the importance of the midregion fragment, hPTH(28–48), for creatine kinase activitiy and DNA synthesis in skeletal tissues has been demonstrated (Sömjen et al., 1990, 1991), while the C-terminus, hPTH(53–84), contains a region that influences alkaline phosphatase activity in osteoblastic cells (Murray et al., 1989; Murray, 1992; Baba, 1992). In addition, these two regions are also essential for the processing and secretion of the hormone (Baba, 1992; Lim et al., 1992). With a view to understanding the physiological role of the intact hormone, a knowledge of its secondary and tertiary structure in solution at the atomic level is of prime importance. Although such detail for the hormone has to date not been possible, an early study allowed a model of the global structural features of bPTH to be made from dark-field electron microscopy (Fiskin et al., 1979). The presence of recurring images suggested that the molecule is comprised of two interconnected domains of different masses of specific orientation one to the other. Secondary structure predicted by the Chou–Fasman algorithm was then fitted into the three-dimensional structure. A similar

* Correspondence should be addressed to this author at the Abteilung für Molekulare Strukturforschung, GBF—Gesellschaft für Biotechnologische Forschung, Mascheroder Weg 1, D-38124 Braunschweig, FRG. Tel: 531-6181-362; FAX: 531-6181-355.

‡ Abteilung für Molekulare Strukturforschung.

§ Abteilung für Genetik.

‖ Arbeitsgruppe für Peptid Synthese.

® Abstract published in *Advance ACS Abstracts,* February 1, 1994.

[1] Abbreviations: bPTH, bovin parathyroid hormone; CD, circular dichroism; COSY, correlation spectroscopy; hPTH, human parathyroid hormone; hPTHrP, human parathyroid hormone-related peptide; NMR, nuclear magnetic resonance; NOE, nuclear Overhauser enhancement; NOESY, nuclear Overhauser and exchange spectroscopy; RMS, root mean square; TFE, trifluoroethanol; TOCSY, total correlation spectroscopy.

0006-2960/94/0433-1684$04.50/0

model, different in specific details but with the same global features, was derived semiempirically from various prediction schemes combined with available chemical data (Zull & Lev, 1980). It is only recently, with the possibility of using high-field NMR spectroscopy, that the acceptability of such models can be probed. It has also become apparent from detailed CD and NMR studies that the solution conditions, and hence the molecular environment in the vicinity of small proteins such as hormones and neurotransmitters, play a significant structural role. This must be taken into account as the main mode of action of PTH is mediated through interaction with a membrane-bound G-protein-coupled receptor (Jüppner et al., 1991).

In keeping with several earlier studies on N-terminal fragments (Bundi et al. 1976, 1978; Lee & Russell, 1989) and our initial study of recombinant prolyl-hPTH(1–84) by ^{1}H NMR and CD spectroscopy, we found that there was very little evidence of stable secondary structure in aqueous solution and that, only on the addition of trifluoroethanol (TFE), was a significant α-helical content observed (Klaus et al., 1991). This was confirmed by CD studies of hPTH and several deletion analogues, which showed that α-helix formation occurred mainly in the 1–34 region (Neugebauer et al., 1992). In the same study, detailed CD investigations of this region using N- and C-terminal analogues suggested the helix corresponding to residues 17–29 was stabilized by addition of 10–20% TFE, while a second helix comprising residues 3–11 was stabilized by addition of slightly higher concentrations of TFE. For hPTH(1–34) and bPTH(1–34) increasing amounts of TFE (up to 45% TFE) caused the helical content to increase up to a steady state in which 24–26 residues were involved [Neugbauer et al. (1992) and Cohen et al. (1991), respectively]. A similar phenomenon was noted for hPTHrP(1–34), which has 8 of the first 13 N-terminal residues in common with hPTH(1–34) (Cohen et al., 1991). From the combination of these CD results, secondary structure predictions, and the observation of several long-range ^{1}H nuclear Overhauser enhancements between protons in the N-terminal and C-terminal residues of hPTHrP(1–34) (Barden & Kemp, 1989), a model has been proposed for both this peptide and hPTH-(1–34) in which there is close contact between the N- and C-terminal helices along their hydrophobic surfaces (Cohen et al., 1991). Although our own detailed studies of hPTH-(1–34) in 10% TFE solutions using ^{1}H NMR spectroscopy did indeed show the positions of two helical regions in the molecule at positions 3–9 and 17–28 joined by a nonstructured region, we could find no evidence of any form of interaction between the helices (Klaus et al., 1991). A recent study of the same fragment (Barden & Cuthbertson, 1993), again in 10% TFE, has essentially duplicated and confirmed our earlier findings. Similarly, in more recent work on [Ala^{26}]hPTHrP-(1–34) there is no specific mention of interactions between the N-terminal helix and the C-terminal structured region (Ray et al., 1993).

Hence, as TFE in concentrations greater than 10% appear to affect at least the secondary structure content, we have investigated the structure of hPTH(1–34) in 70% TFE by ^{1}H NMR spectroscopy specifically with a view to understanding the effect of TFE on the development of helical content and the possibility of helix–helix interactions. During the preparation of the present manuscript and after completion of the experimental work on hPTH(1–34) (Federau, 1992), a study of this fragment in 40% TFE by NMR spectroscopy has appeared (Strickland et al., 1993) which extends our original work and complements the results presented here for solutions in 70% TFE. The structures in both solutions are quite similar, and this is considered more fully below.

In a continuation of our studies and as an approach to the structure of the intact hormone, we have investigated various biologically relevant fragments of hPTH corresponding to the central [hPTH(18–48) and hPTH(28–48)] and C-terminal [hPTH(53–84)] regions under a variety of solution conditions to ascertain their potential for forming secondary and tertiary structures. Again TFE was chosen in order to mimic, as far as possible, the environment in the vicinity of the membrane-bound receptor, conditions that are completely different from those in aqueous solution alone. Recent work (Sönnichsen et al. 1992) has clearly shown that TFE stabilizes helices only in those regions of the peptide that have a propensity for helical structure and leaves untouched, as flexible regions, those parts that have no such preference. In this paper, we present direct experimental evidence that only specific regions of hPTH have a propensity for secondary structure and that the stability of this depends upon the solution conditions.

MATERIALS AND METHODS

Peptide Synthesis. The four hPTH sequences 1–34, 18–48, 28–48, and 53–84 were assembled with a Milligen 9050 peptide synthesizer on NovaSyn PA 500 resins preloaded with the C-terminal amino acids. 1-Fluorenylmethoxycarbonyl amino acids were used throughout the syntheses in a 3-fold excess and activated with 2-(1*H*-benzotriazol-1-yl)-1,1,3,3-tetramethyluronium tetrafluoroborate and diisopropylethylamine in equal molar ratios. Serine, threonine, aspartic acid, and glutamic acid were *tert*-butyl protected, lysine with *tert*-butyloxycarbonyl, asparagine, glutamine, and histidine with trityl, and arginine with 2,2,5,7,8-pentamethylchroman-6-sulfonyl. For deprotection and isolation of the peptides the dried resins were treated for 3 h with trifluoroacetic acid containing 3% triisobutylsilane, and 2% water (10 mL/g of resin). The resins were removed by filtration and washed with acetic acid, and the combined filtrates and washings were evaporated to near dryness. *tert*-Butyl methyl ether was added, and the precipitates were collected by centrifugation. After two resuspensions in ether and centrifugations, the precipitates were dried, dissolved in water/acetonitrile (1:1), and passed over octadecyl disposable extraction columns. After rinsing the columns with acetonitrile, most of the acetonitrile of the eluents was evaporated. The aqueous solutions were lyophilized and the resulting crude peptides purified by preparative reversed-phase HPLC. Analyses by fast atom bombardment mass spectrometry and gas-phase sequencing gave the expected results. In all cases the C-terminal acid was synthesized.

Sample Preparation, CD, and NMR Spectroscopy. Samples of each peptide were dissolved in distilled water, and then the appropriate volume percentage of TFE was added to give a final concentration of 0.1 mg mL^{-1}. CD spectra were recorded at room temperature on a Jasco J-600 spectropolarimeter (Jasco, Tokyo, Japan), at wavelengths between 184 and 260 nm, using a cuvette with a path length of 1 mm. Secondary structure elements present in solution were quantified by the use of the program VARSELEC (Hennessey & Johnson, 1981).

For the NMR measurements samples of each peptide (3 mg) were dissolved in distilled water, to which the appropriate volume percentage of TFE-d_2 [produced by fractional distillation of a 1:1 mixture of H_2O and the TFE-d_3 (Merck, Darmstadt, Germany)] was added to give a final volume of 0.6 mL. 1D and 2D ^{1}H NMR spectra were recorded on a

Bruker AM 600 NMR spectrometer without spinning, using a dedicated 5-mm proton probe head and an external temperature control (Haake GmbH, Karlsruhe, Germany). All 2D phase-sensitive COSY, TOCSY (mixing time 70 ms), and NOESY (mixing time 150 ms) spectra were recorded and processed, and cross-peaks in the latter were integrated as described previously (Wray et al., 1993). All spectra were referenced to the residual signal of water or the methylene protons of trifluoroethanol relative to 3-(trimethylsilyl)-propanesulfonic acid sodium salt (0.00 ppm), under the appropriate experimental conditions.

Signal Assignments. In all cases a standard strategy for structure elucidation by ^{1}H NMR spectroscopy was used (Wüthrich, 1986) that has been described in detail by us elsewhere for hPTH(1–34) (Klaus et al., 1991). The complete amino acid spin systems were identified from 2D ^{1}H phase-sensitive COSY and TOCSY spectra, starting from the backbone amide protons in the region 9.0–7.6 ppm, except for proline residues, which were identified from their α-proton signals in the region 4.5–4.0 ppm. Sequence-specific assignments were then determined from the cross-peaks in 2D ^{1}H phase-sensitive NOESY spectra, with mixing times of 150 ms, where NOE signals were observed between H_N, H_α, and H_β of amino acid i and H_N of amino acid $i + 1$. In addition to intraresidue and sequential NOE's hPTH(1–34) and hPTH(18–48) showed a considerable number of medium-range NOE's between H_α of residue i and H_N and H_β of residue $i + 3$ which are characteristic of interactions within α-helices (Wüthrich, 1986). Although few such interactions were observed for hPTH(53–84), which precluded the presence of helix in this fragment, several longer-range interactions were observed between protons of residues more than 3 residues apart in the sequence and indicated tertiary structure formation in this fragment. The assignments and chemical shift data for the fragments are presented as supplementary material.

Structure Calculations. The volumes of the integrated cross peaks from the NOESY spectra (150 ms) were determined by using the AURELIA program (Niedig & Kalbitzer, 1990) and calibrated against those of side-chain amide protons (0.19 nm). After correction for pseudoatoms and methyl groups, where appropriate, these values were used directly as distance restraints in distance geometry calculations with the program DISGEO (Havel & Wüthrich, 1984). The best of these were then subjected to energy minimization and molecular dynamic simulations using the program XPLOR-version 2.1 (Brünger et al. 1986). The hardware, procedure, and protocol used to obtain the final refined structures that were compatible with the quantitative NOE data have been described previously (Wray et al., 1993). The input data and the number of distance geometry and final restrained molecular dynamic calculations performed are given in Table 1.

Table 1: Input Data Used, and Number of Distance Geometry and Final Restrained Molecular Dynamic Calculations Performed

peptide	no. of NOE's used[a]	no. of DG	no. of MD[b]	superposition	av RMS deviation (nm)[c]
PTH(1–34)	146 (43, 69, 34)	500	7	3–13	0.114
				15–26	0.137
PTH(18–48)	145 (25, 76, 40)	317	9	21–28	0.073
				29–38	0.078
PTH(53–84)	188 (88, 79, 21)	40	7	55–84	0.230

[a] These quantitative NOE's were used as distance restraints in the DG and MD calculations. The values in parentheses correspond to the number of intraresidue, sequential, and medium-range [plus long-range for PTH(53–84)] NOE's, respectively. [b] For hPTH(1–34) and hPTH(18–48) all final restrained MD structures had $E(\mathrm{NOE})_{tot}$ less than 61 kJ mol^{-1} for a NOE force constant of 13 440 kJ·nm^{-2}·mol^{-1}. [c] The RMS deviation analysis used all the backbone atoms of the residues superimposed, and each structure was compared with every other structure.

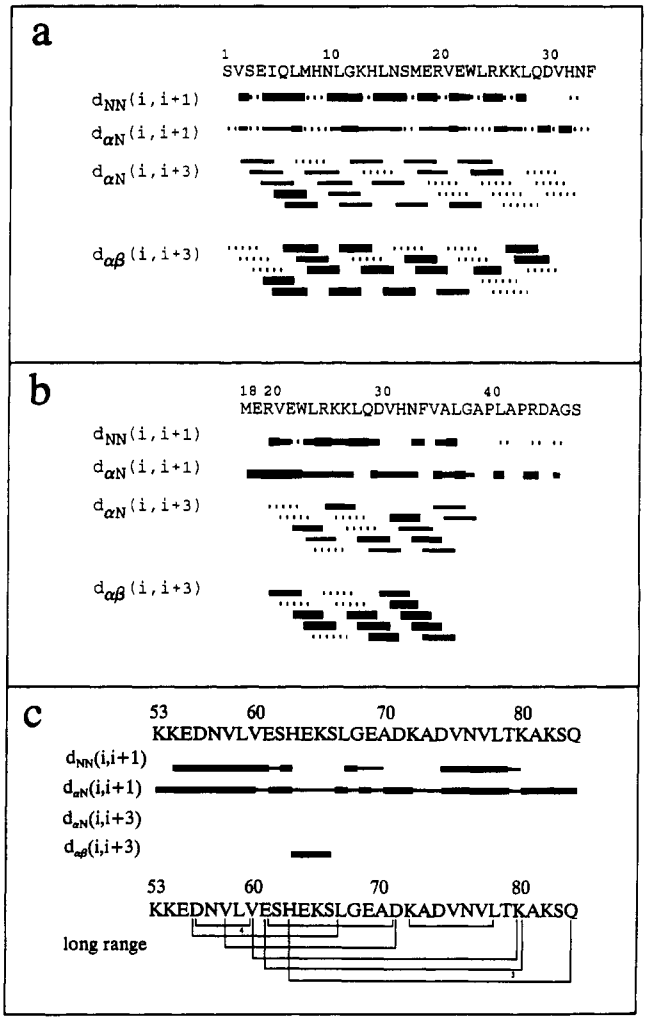

FIGURE 1: Summary of observed NOE's for (a) hPTH(1–34) in 70% TFE, (b) hPTH(18–48) in 50% TFE, and (c) hPTH(53–84) in 10% TFE. The weakly shaded areas in (a) and (b) correspond to NOE's that were not observed, but are probably present, in the NOESY spectra because of signal overlap. These signals were not included in the structure simulations. For (c) only the signals observed that were used in the structure simulations are shown. For the long-range NOE's each line corresponds to one interaction between the shown residues, except for Asp-56 with Val-60 and Glu-61 with Lys-80, where 4 and 3 separate interactions were observed, respectively.

RESULTS

Structure of hPTH(1–34). As a continuation of our study of hPTH(1–34) we have recorded ^{1}H NMR spectra in aqueous 70% TFE as this should be a solution in which a limiting helical structure, involving 24–26 residues, has been reached according to CD measurements (Neugebauer et al., 1992). The quantitative NOE data are shown in Figure 1a. Under these solution conditions there was considerable signal overlap, which prevents the detection of a number of medium-range NOE's, as noted in Figure 1a. In spite of this a satisfactory set of conformations could be calculated from the quantitative NOE data, which after alignment for minimum RMS error possessed the features shown in Figure 2. After an initial disordered region of two residues there are two well-defined α-helices from Ser-3 to Lys-13 and from Leu-15 to Lys-26, between which there is a region that can access several conformations. The structures found here are similar to those

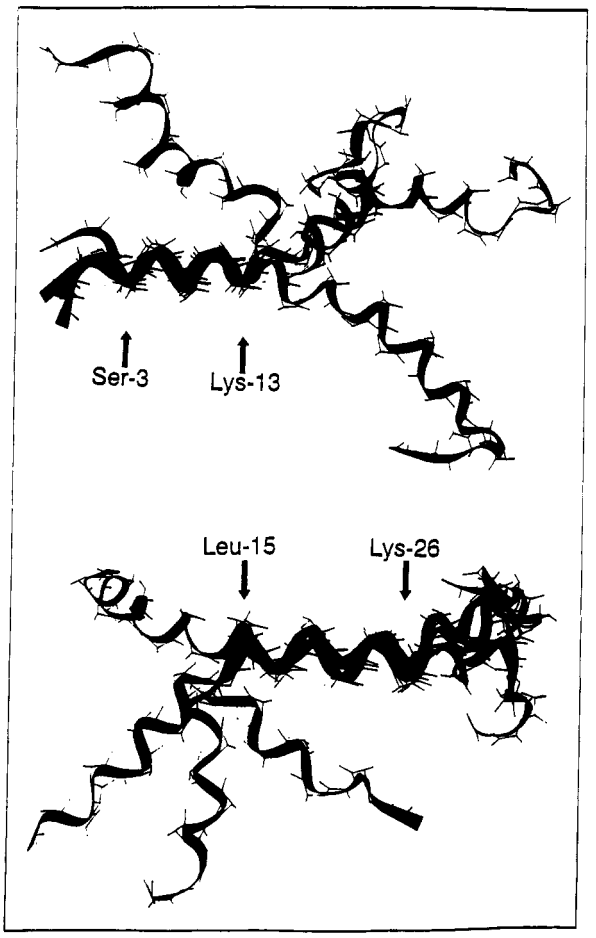

FIGURE 2: Superpositions of four final restrained MD structures after fitting of the backbone atoms C_α, C, and N of Ser-3 to Lys-13 (upper) and Leu-15 to Lys-26 (lower) of hPTH(1–34) in 70% TFE.

found in 40% TFE (Strickland et al., 1993), where two helices were detected spanning residues 3–12 and 17–26 joined by a region that possessed ordered conformations but could not be described by a single set of conformations. Our data are more compatible with this section possessing an ordered structure in which the helices only show a short discontinuity between residues 13 and 15. It is probable that in 70% TFE the section containing residues 12–17 is further stabilized in a helical conformation. This would appear to be the case. In 40% TFE there are no NOE's $d_{\alpha N}(i,i+3)$ for H_α involving residues 13–16, while in 70% TFE these are observed for 14/17 and 16/19 (Figure 1a).

That the discontinuity between Lys-13 and Leu-15 in our structure is a genuine characteristic of the fragment is confirmed from the experimental data, as several crucial NOE's, $d_{\alpha\beta}(i,i+3)$ for residues 12/15 and $d_{\alpha N}(i,i+3)$ for 15/18, are absent and lie in a region of the spectrum where there is no overlap. In contrast, the experimental observation of $d_{\alpha\beta}(i,i+3)$ for 26/29 and 27/30 and the inability to observe several relevant NOE's in the region Lys-26 to Asp-30 due to signal overlap are an indication that in reality the helix may continue to residue 29 or 30. This is confirmed by the chemical shift observations discussed below. A careful inspection of the complete 2D NOESY spectrum showed no evidence of long-range NOE's between the two helical regions. An absence of such NOE's has also been noted in less concentrated TFE solutions (Klaus et al., 1991; Strickland et al., 1993).

It has been shown that the α-proton chemical shifts are dependent on the nature and character of protein secondary

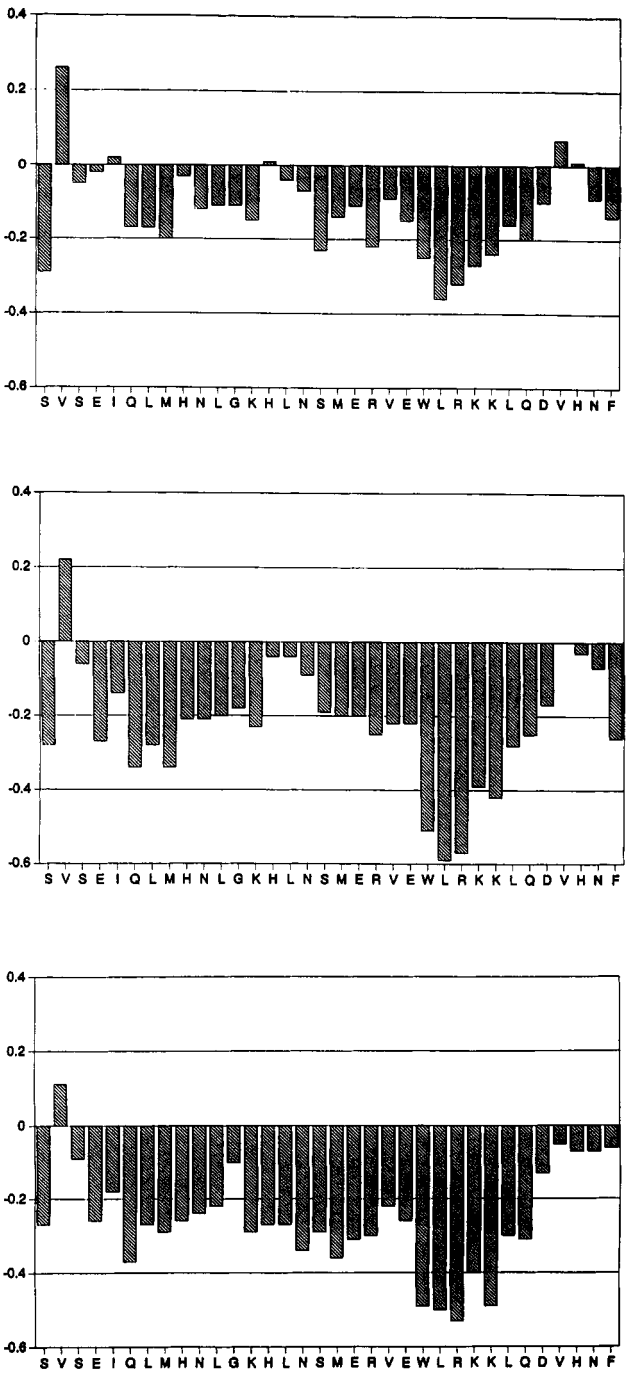

FIGURE 3: Chemical shift differences of the α-protons of hPTH-(1–34) in 0% TFE [upper; data from Lee and Russell (1989)], in 10% TFE [middle; data from Klaus et al. (1991)], and in 70% TFE (lower; data from present work).

structure (Wishart et al., 1992), such that upfield shifts relative to the random coil values are found for residues in α-helices and downfield shifts for those in β-sheets. Provided a minimum number of adjacent residues (3 for β-strand and 4 for α-helix) show shifts greater than 0.1 ppm, then the data furnishes a simple, reliable method of assessing protein secondary structure. Recently, we have confirmed that this method is also applicable to small peptides in aqueous TFE solutions (Wray et al., 1993). In the present case the plot of the α-proton shift differences in 70% TFE (Figure 3, lower) confirms the existence of helical secondary structure between residues 4 and 29 with a possible loss of helical character in the region of Gly-12. Comparison of this data with our earlier data in 10% TFE (Figure 3, middle) and with that in aqueous solution

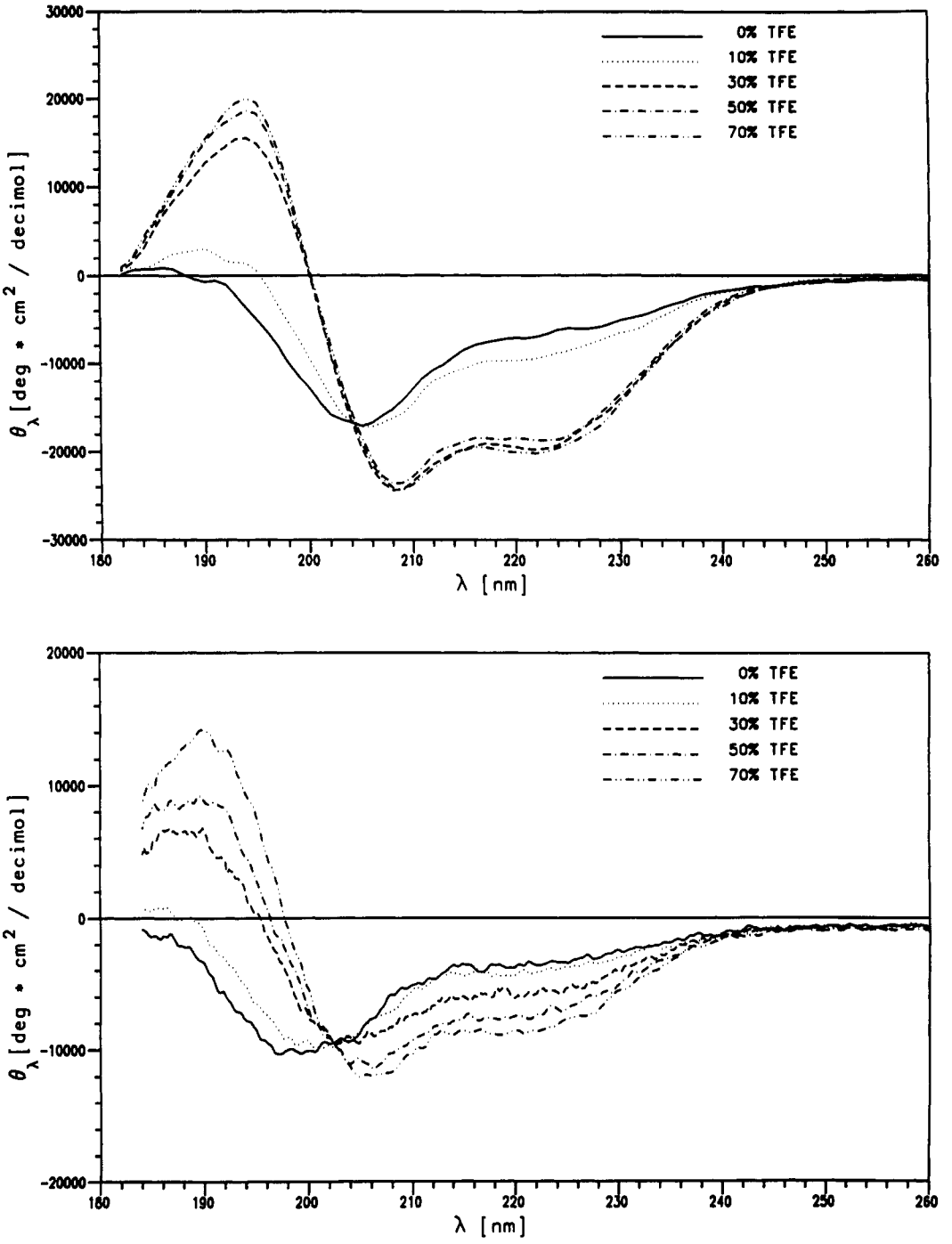

FIGURE 4: CD spectra of hPTH(18–48) (upper) and hPTH(53–84) (lower) in aqueous solution containing TFE.

(Figure 3, upper) is instructive. Using the criteria of Wishart et al. (1992) for the detection of secondary structure, hPTH-(1–34) initially only shows evidence of weak helical structure in the region 23–27 in aqueous solution in keeping with conclusions of an early NMR study (Bundi et al., 1976). On addition of 10% TFE, the shift differences for this region are more pronounced, indicating the helix is more stable and extends back to ca. residue 16. A second helix is also apparent in the N-terminus starting at Ser-3. Again these features were confirmed from an analysis of the quantitative NOE data and molecular dynamic simulations (Klaus et al., 1991). Finally, addition of more TFE (70%) causes further lengthening and stabilization of the two helices such that the flexible "hinge region", observed in 10% TFE between residues 10 and 17, is less pronounced. From the shift data the region 23–27 appears to have helical character under all solution conditions and is the most stable, least flexible, region of this molecule.

Structure of hPTH(18–48) and hPTH(28–48). As expected, the CD spectrum of hPTH(18–48) in aqueous solution shows only a small amount of α-helix, which increases on the addition of TFE, with the curves becoming more characteristic of helical secondary structure (up to a maximum at 30% TFE, and thereafter showing no change; Figure 4, upper). Deconvolution of these spectra gives 10% (3 residues) helical content in aqueous solution, 30% (9 residues) in 10% TFE, and 70% (19 residues) in the limiting structure.

As with our studies of hPTH(1–34) ^{1}H NMR spectra were recorded and analyzed in 10% TFE and under limiting conditions in 50% TFE. Again the α-proton chemical shift

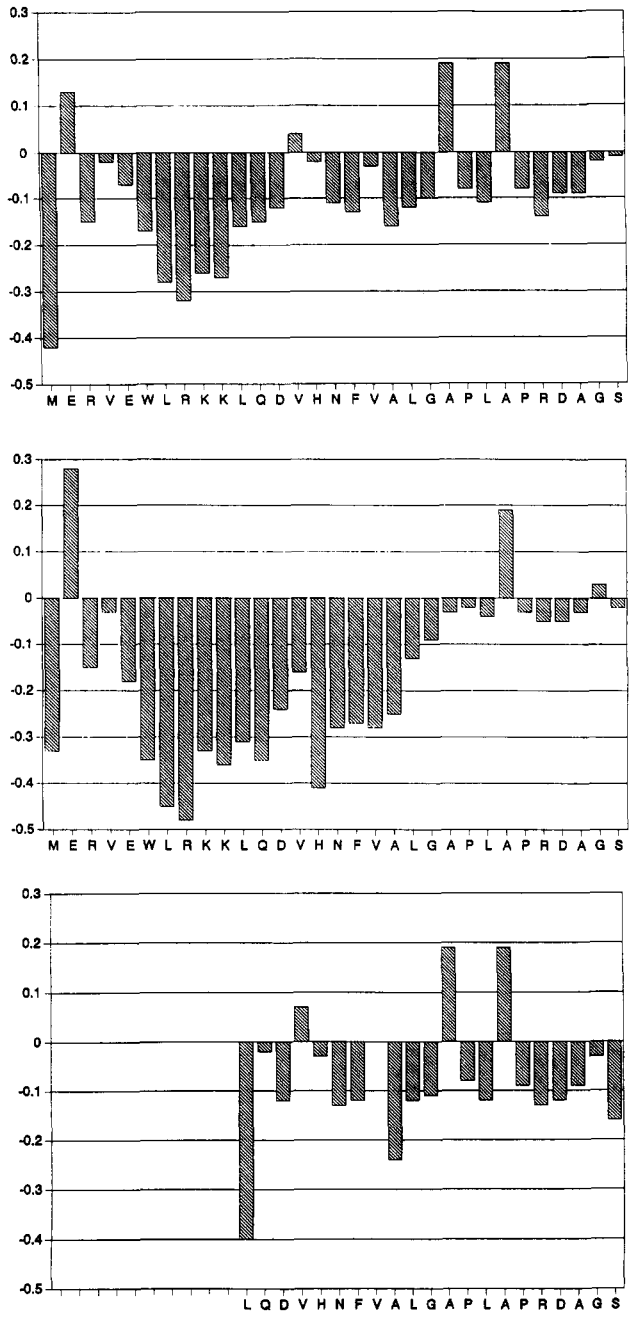

FIGURE 5: Chemical shift differences of the α-protons of hPTH-(18–48) in 10% TFE (upper) and 50% TFE (middle), and of hPTH-(28–48) in 10% TFE (lower; chemical shift data is not tabulated).

provides information as to the extent and position of secondary structure. In keeping with the CD data in 10% TFE 6–8 residues are present as α-helix in the region 23–30 (Figure 5, upper), while in the limiting structure in 50% TFE this extends into the central section of the molecule as far as Gly-38 (Figure 5, middle). From this residue to the C-terminus of the fragment there is no structure apparent, with the shifts showing little deviation from the random-coil values. Again residues 23–27 appear to sustain helical structure more readily than the rest of the molecule. An analysis of hPTH(28–48) in 10% TFE supports these observations as there was no evidence of regular secondary structure in the α-proton chemical shift difference plot (Figure 5, lower).

The NOE data for hPTH(18–48) in 50% TFE (Figure 1b) confirm the presence and extent of the helix, and the quantitative data, after distance geometry and molecular dynamic simulations, afford the set of conformations shown

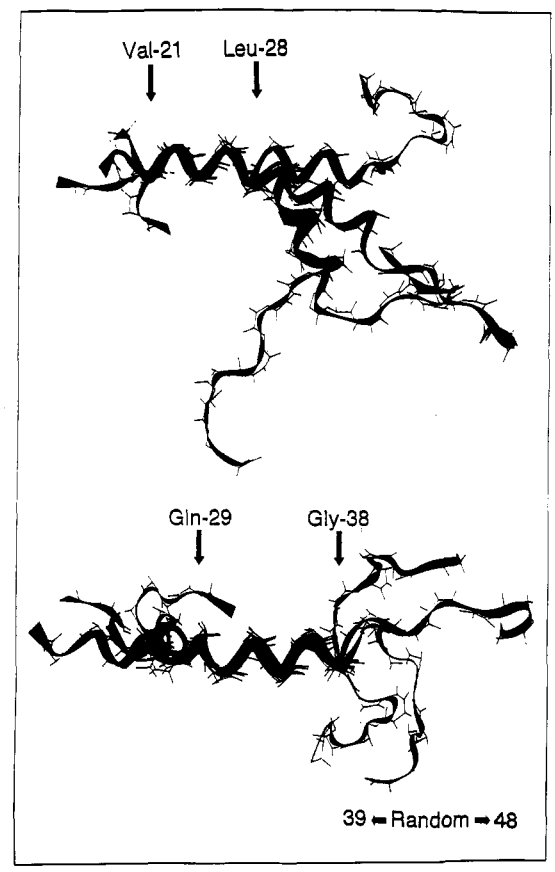

FIGURE 6: Superpositions of four final restrained MD structures after fitting of the backbone atoms C_α, C, and N of Val-21 to Leu-28 (upper) and Gln-29 to Gly-38 (lower) of hPTH(18–48) in 50% TFE. No superimposable structures were found in the region Ala-39 to Ser-48.

in Figure 6 after superposition analysis. A well-defined helix extents from Val-21 to Gly-38, with a discontinuity between Leu-28 and Gln-29. The helix terminates at Gly-38, and there is no stable structural element in the C-terminus. The discontinuity is not apparent in all nine final conformations (Figure 6) and may arise from the limited number of medium-range NOE restraints, due to signal overlap, available for this region of the molecule. Unlike the same feature (residues 13–15) in hPTH(1–34) above, the absence of $d_{\alpha\beta}(i,i+3)$ and $d_{\alpha N}(i,i+3)$ NOE's could not be verified, although an unusual $d_{N\beta}(i,i+3)$ NOE between residues 28 and 31 was observed. Hence any interpretation of this feature must be treated with caution.

Structure of hPTH(53–84). The changes in the CD curves of hPTH(53–84) on addition of TFE (Figure 4, lower) are less pronounced than those of hPTH(18–48), and a more gradual change with increasing TFE content is observed, suggesting that the limiting structure is only achieved at the highest TFE concentrations used. Deconvolution of the spectra indicate a gradual increase from 10% helical content in aqueous solution to 25% in 70% TFE, corresponding to involvement of 3 and 8 residues, respectively. Currently, ^{1}H NMR data are available for 10% TFE solutions. Not surprisingly, the α-proton chemical shift difference plot (Figure 7) shows no evidence of α-helix, and it is only from the medium-range NOE data (Figure 1c) that there appears to be helix or turns in the N-terminus of the fragment. Several further medium- and long-range NOE's (Figure 1c) are indicative of a loose tertiary structure. These quantitative NOE's were used as distance restraints in distance geometry and restrained molecular dynamic simulations to give a set of conformations

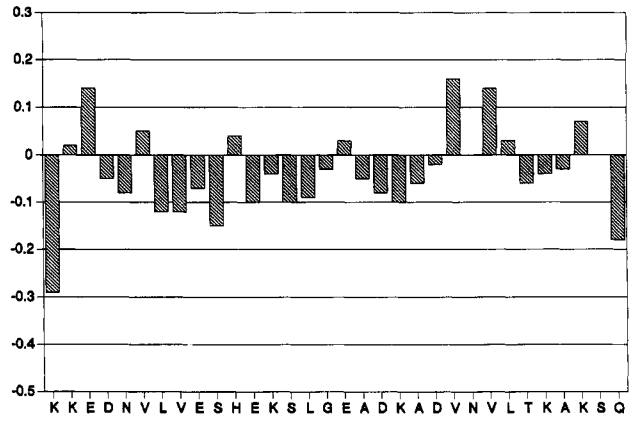

FIGURE 7: Chemical shift differences of the α-protons of hPTH-(53–84) in 10% TFE.

compatible with this data (Figure 8). Although the refined structures are not as well-defined as the helices of the other fragments (Table 1), it is clear that this fragment is the only fragment that adopts any form of tertiary structure under these solution conditions. There is an initial series of close turns within the first 15 residues that create a relatively compact nucleus. The remaining residues adopt a more open loop structure surrounding the initial series of turns to which they are anchored in two regions, defined by the long-range NOE's (Figure 1c), between residues 60–64 and residues 80–84, and between residues 58–61 and residue 71. It is these interactions that impart a more compact structure to this fragment. The absence of medium- and long-range NOE's within the region 72–78 indicate that this is the most flexible loop in the peptide and can adopt a number of widely differing conformations. At high concentrations of TFE, it is probable that the initial residues adopt a more helical conformation.

DISCUSSION

In an attempt to gain an immediate insight into details of the structure of intact hPTH, we have chosen to look at the structure of various fragments of the molecule that have been shown to be of biological interest. As these in effect cover the whole hormone, this study gives details of the entire structure and shows the variations that occur under various solution regimes. It is now clear from our initial NMR study of the 34 amino acid N-terminus (Klaus et al., 1991), and from several CD studies of this and related peptides (Zull et al., 1990; Cohen et al., 1991; Neugebauer et al., 1992; Strickland et al., 1993), that the structure adopted by such molecules is strongly dependent upon their environment, such that they display different structural properties under different solution conditions. This is probably an important characteristic trait of small peptide hormones that act through binding to membrane-bound receptors, as it is found for many such systems (Kaiser & Kézdy, 1987).

The CD spectra of hPTH(18–48) show little evidence of extensive secondary structure in aqueous solution (Figure 4, upper), in agreement with the CD spectra of several PTH analogues (Neugebauer et al., 1992). Addition of TFE causes stabilization of helix which, from the α-proton chemical shift plots (Figure 5, upper), occurs most readily in the region of residues 23–27. The same region is the first to show shifts characteristic of helix in hPTH(1–34) from the plots of published data (Figure 3) and appears even to be present in 0% TFE. Thus the helical character found in CD studies and estimated to involve 7–9 residues in aqueous solution alone (Cohen et al., 1991; Neugebauer et al., 1992) appears to be situated in the second helical region centred at residues 23–27. This is borne out by the observation in time-resolved fluorescence studies of a local helical structure around Trp-

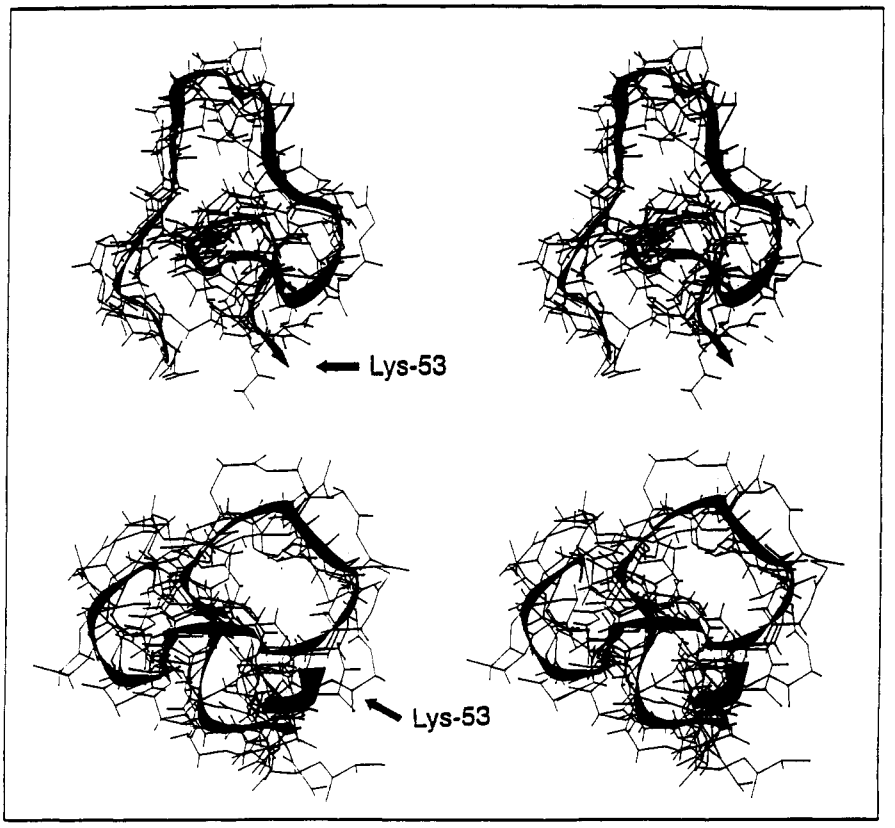

FIGURE 8: Stereoview superpositions of six final restrained MD structures after fitting of the backbone atoms C_α, C, and N of the entire fragment of hPTH(53–84) in 10% TFE. The lower set corresponds to the upper viewed from below.

23 in aqueous solutions of hPTH and hPTH(1–34) (Willis & Szabo, 1992) and is in keeping with the observation that less TFE is required to stabilize the second helical region than the first shorter N-terminal one (Neugebauer et al., 1992). In a very recent study of hPTH(1–34) in aqueous solution without TFE (Barden & Kemp, 1993) rather well-defined α-helical regions have been found in larger proportions than expected from the above. Indeed, in contrast to earlier work (Lee & Russell, 1989) a remarkable number of NOE's have been observed. Although it is possible that the structural calculations from the NOE data may overestimate the helical content, the results do show that the second helix in the region Val-21 to Gln-29 is better defined than that in the N-terminus. These conclusions are at variance with a model proposed by Zull et al. (1990) of a more stable initial helical region between residues 6–12 in aqueous solution, which has been criticized more fully elsewhere (Willis & Szabo, 1992), and are also incompatible with the tentative conclusions of a theoretical study using a Monte Carlo simulated annealing protocol (Okamoto et al., 1993).

The α-proton chemical shift changes caused by addition of TFE to solutions of hPTH(1–34) (Figure 3) are evidence of an extension of the helices into the flexible hinge region found in 10% TFE. From the simulations using the quantitative NOE data in the limiting case of 70% TFE, the first two residues are always conformationally free and there is still a discontinuity between the two helices at residues 13–15 (Figure 2). As a consequence, the conformational possibilities of the helices one with respect to the other are severly restricted compared to those in 10% TFE. The absence of any long-range NOE's under these solution conditions precludes a stable interaction between the two helical regions and is compatible with the fact that there is no evidence of such structures among the seven final conformations after restrained molecular dynamic simulations. Support for these conclusions is afforded by our earlier studies of hPTH(1–34) in 10% TFE and by recent studies of a hPTHrP(1–34) mutant (Ray et al., 1993) in 30% TFE, where in both cases no long-range NOE's were documented. Fluorescence studies of hPTH(1–34) also showed that there was no evidence of extensive interactions between the two helical regions, as the data suggest that Trp-23 is solvent exposed (Willis & Szabo, 1992). Thus in solutions containing TFE there are no helix–helix interactions.

The situation for hPTH(1–34) and hPTHrP(1–34) in water alone remains somewhat confused as ^{1}H NMR studies at 400 MHz of hPTHrP(1–34) appeared to show long-range NOE's consistent with interactions of the N- and C-terminal residues (Barden & Kemp, 1989). Similar interactions were not found recently in hPTH(1–34), although unusual long-range interactions were found within the C-terminal half of the peptide (Barden & Kemp, 1993). As small differences in the experimental conditions (such as pH, peptide concentration, and salt content) are unlikely to affect the observations of long-range interactions, one must currently conclude that even small amounts of TFE disrupt such interactions with a preference for helix stabilization. However, as noted above, these same studies suggest an unusual amount of stabilized helical content in contrast to both CD and earlier NMR studies and also are in contrast with the results here for hPTH(18–48), where there is little evidence of helix from CD measurements in water alone (Figure 4).

The extent of the second helix in hPTH(1–84) can better be judged from the limiting structure of hPTH(18–48) in 50% TFE (Figure 6). Here there is a regular helix that starts at Val-21 and ends at Gly-38, with an apparent discontinuity between residues 28 and 29. Increased flexibility and a weakening of the helix at this point would explain the loss of helical character in the C-terminus of hPTH(1–34).

The behavior of hPTH(53–84) is quite different to that of the other larger fragments. According to the CD measurements addition of TFE causes only a small increase in helical content with a maximum involvement of ca. 8 residues at 70% TFE. This is in sharp contrast to the other fragments of similar length. For instance, hPTH(18–48) has an estimated 19 residues in helical structures in 70% TFE and hPTH(1–34) 26 residues in 40% TFE (Neugebauer et al., 1992). Again in contrast to the other fragments the 2D NOESY spectra in 10% TFE showed a number of long-range interactions that allowed characterization of the loose tertiary structure shown in Figure 8. Not unexpectedly, the average RMS deviation for alignment of the contributing conformations is higher for this structure (0.23 nm) than for the partial regular helical structures of the other fragments (0.07–0.14 nm), reflecting not only the greater flexibility but also the larger number of aligned residues. Apart from the first two conformationally labile residues the N-terminus of hPTH(53–84) assumes an initial tight series of turns over which the rest of the molecule folds. The C-terminus is anchored to the compact N-terminus in two regions through interactions of residues in the region 58–64 (N-terminus) with residue 71 and residues 80–84. The most flexible region of the molecule is found in the loop region 72–78, where there is no evidence of stabilizing interactions with other regions of the molecule.

Thus, combining the information from the four fragments, the limiting structure of hPTH(1–84) in a "membrane-like" environment simulated by TFE is shown in Figure 9. Of course, this structure is unable to provide information of the interfragment interactions that may lead to teriary structure in the intact protein. The present structural details are compared schematically with a summary of the wide-ranging literature on the biological activities of the hormone and its various fragments. We have attempted to be comprehensive, although clearly only those investigations where attempts at defining activities to specific regions of the hormone have been included. Even then, only a much simplified graphic showing broad correlations can be presented. For more detailed information the reader is referred to the figure caption and the references cited therein.

The hormone can be divided into two terminal regions of approximately equal size, in which there are defined structural features, joined by a central flexible, nonstructured linker. Helical secondary structure is the major feature in the N-terminus, while in contrast the C-terminus has very little helix and is dominated by a loosely folded structure. Noticeably, the predominant helix in the N-terminus contains a region that is present under most solution conditions (23–29) and contains a section which is amphiphatic in character (21–37) and is stabilized both in TFE and in lipid solution (Neugebauer et al., 1992). It is this region that is responsible both for binding to the membrane-bound G-protein-coupled receptor for adenylate cyclase and phospholipase C activity, and would undoubtedly be in a helical conformation in such an environment. Although nothing is known structurally about the hormone–receptor interaction, it is possible that the helix region is long enough to span the membrane and could potentially interact with a pocket formed by the seven helical membrane-spanning domains of the receptor (Jüppner et al., 1991). This is in keeping with a hypothesis of Potts, that the hormone must enter the plasma membrane to allow certain intramembranous regions on the receptor to be contacted for

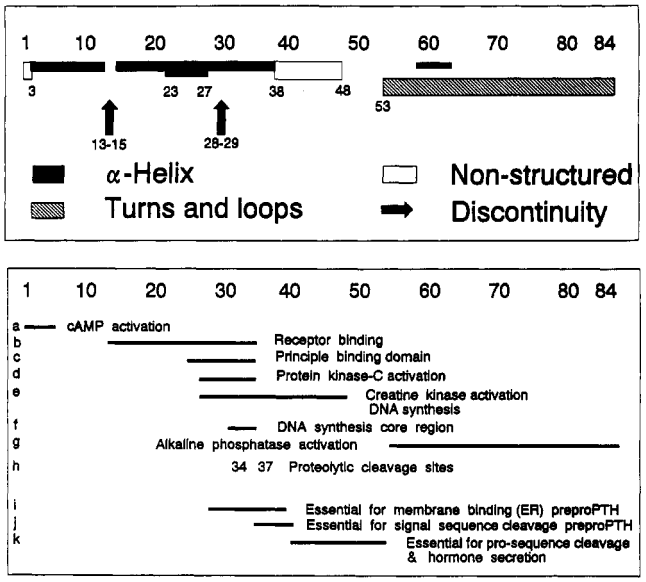

FIGURE 9: (A, upper) Summary of the main structural features of hPTH(1–84) in a "membrane-like" environment taken from the structures of four fragments [hPTH(1–34), hPTH(18–48), hPTH-(28–48), and hPTH(53–84)] in TFE solution. The nature of the region 48–53 has not been covered by the present study. The interpretation of the discontinuity between residues 28 and 29 must be treated with caution (see text). (B, lower) Schematic of the biological properties of hPTH(1–84) and related molecules from the current literature. The literature is summarized according to the lower case letters to the left in panel B (lower panel) followed by the residues involved and a short description with the reference: (a) 1–4: Important for cAMP activity [cf. for review Gardella et al. (1991)]. 1 and 2: Required for activation of cAMP in renal cortical cells (Takano et al., 1988) and cAMP/protein kinase A activation in osteosarcoma cells (Fujimori et al.,1992). 1: N-terminal Ala in bPTH-(1–34) is important for vasorelaxant activity in rat tail artery strips, which is reduced when Ser is present. In this context it would appear that the active core, bPTH(24–28), is also important (Chiu et al., 1992). 3 and 6: Contribute to PTH binding and activation of adenylate cyclase in kidney and bone (Cohen et al., 1991). 8: Oxidation of Met-8 in bovine PTH(1–34) shows this residue is implicated in activation of adenylyl cyclase and binding (Frelinger & Zull, 1986). (b) 14–34: Receptor binding domains of PTH and PTHrP in bovine renal cortical membrane and rat osteosarcoma cell binding and cAMP assays (Caulfield et al., 1990). 13–17: Lactam formation (with helix stabilization) in PTHrP(7–34) gives 5–10-fold more potent receptor binding in PTH-stimulated adenylate cyclase assays than parent (Chorev et al. 1991). 18: Oxidation of Met-18 in bPTH(1–34) shows this residue is implicated only in binding (Frelinger & Zull, 1986). 12: Exchange of flexible Gly-12 with hydrophobic residues was well tolerated and led to antagonists that were 10-fold more active antagonists than 7–34 parent PTH (Chorev et al. 1990). For summary, see Caulfield and Rosenblatt (1990). (c) 25–34: Deletion studies have shown that this region is the principle binding domain in bone and kidney cells (Nussbaum et al., 1980), in particular, Leu-24, Leu-28, and Val-31 are the residues of importance (Gardella et al., 1993). (d) 28–34: Membrane-associated protein kinase C activation (Jouishomme et al., 1992). (e) 28–48: Causes increased creatine kinase activity and DNA synthesis *in vitro* and *in vivo*, but has no effect on cAMP activity. Inhibits the increase in cAMP of bPTH-(1–84) (Sömjen et al., 1990, 1991). (f) 30–34: DNA synthesis core region in cell cultures of chicken chondrocytes (Schlüter et al., 1989). (g) 53–84: Influences alkaline phosphatase activity in dexamethasone-treated rat osteoblastic osteosarcomic cells (Murray et al., 1989; Murray, 1992; Baba, 1992). (h) 34 and 37: Proteolytic cleavage in the liver *in vivo* occurs principally between residues 33/34 and 36/37 [for review see Potts et al. (1982)]. 38: Anomalous cleavage by staphyococcal protease between residues 38/39 (Segre et al., 1977). (i) 28–39: Essential for membrane binding (ER) in preproPTH (Baba, 1992; Lim et al., 1992). (j) 34–40: Essential for signal sequence cleavage in preproPTH (Baba, 1992; Lim et al., 1992). (k) 40–52: Essential for prosequence cleavage in proPTH and hormone secretion (Baba, 1992; Lim et al. 1992).

effective binding (Potts, 1992). Interestingly, residues 1–4, which are crucial for receptor activation, lie outside this region in a part of the molecule that remains flexible under all solution conditions. This global activation/binding motif requires only the first 34 residues and is also found for a number of other cAMP-stimulating peptide hormones, such as the secretin family (members include secretin, glucagon, growth hormone-releasing factor 1–29, vasoactive intestinal peptide, pituitary adenylate cyclase-activating polypeptide, and helodermin) (Wray et al., 1993) and calcitonin. Although there is no significant sequential homology between hPTH(1–34), calcitonin, and the secretin family of neuropeptides, the G-protein-coupled receptors appear to be strikingly similar both in predicted secondary/tertiary structure and in amino acid identity (Jüppner et al., 1991; Lin et al., 1991; Ishihara et al., 1991). This similarity is such that bPTH(1–84) and hPTH-(1–34) can displace glucagon from the glucagon receptor, even though there is no structural homology between the peptides (Shah et al., 1987).

Such a ready division between binding and activation domains, however, is not apparent for membrane-associated protein kinase C activity (Figure 9Bd) that is also thought to occur via a G-protein-coupled receptor-activating phospholipase C isoenzyme. Here the activation site is located within residues 28–34, while the helix region within residues 13–27 is probably needed for binding (Jouishomme et al., 1992). A further series of processes appear to be stimulated by fragments of the molecule that contain little (Figure 9Be,f) or virtually no helical region (Figure 9Bg), and hence do not or cannot use helix binding interactions. The receptor type in these processes has not been defined (Sömjen et al., 1991).

Membrane binding is also an important function in the processing of the hormone precursor of 115 amino acids (Figure 9Bi), and again helical regions are implicated, in particular, the whole region up to residue 39 (Baba, 1992; Lim et al. 1992).

Thus, in summary, there are broad correlations between structural features in "membrane-like" solutions of TFE (and lipids) with *in vivo* and *in vitro* processes involving activation and binding at the receptor and those involving the precursor hormone. More subtle effects can be expected for substitutions or structural modifications at the discontinuities and ends of the helices. This is indeed the case as exchange of Gly-12 with less flexible hydrophobic residues is well tolerated and gives rise to potent antagonists (Chorev et al., 1990), while lactam formation in the region 13–17 leads to increased receptor binding (Chorev et al., 1991), presumably through helix stabilization. Similarly, the helix end at the center of the molecule is the position of normal and abnormal proteolytic cleavage (Figure 9Bh).

Future structural work will have to concentrate on the intact hormone and its interactions with the receptor(s), while more information is clearly required concerning the function and mode of action of the central and C-terminal regions of the hormone.

ACKNOWLEDGMENT

The authors are grateful to T. Dieckmann and Dr. W. Klaus for useful discussions, and to C. Kakoschke for technical assistance.

SUPPLEMENTARY MATERIAL AVAILABLE

Tables giving the ^{1}H NMR assignments and chemical shifts for hPTH(1–34) in 70% TFE, hPTH(18–48) in 10% TFE, hPTH(18–48) in 50% TFE, and hPTH(53–84) in 10% TFE (6 pages). Ordering information is given on any current masthead page.

REFERENCES

Baba, H. (1992) International Bone Forum: The First International Forum on Calcified Tissue and Bone Metabolism, Yokohama, Japan, 1992, pp 40–43.

Barden, J. A., & Kemp, B. E. (1989) *Eur. J. Biochem. 184*, 379–394.

Barden, J. A., & Cuthbertson, R. M. (1993) *Eur. J. Biochem. 215*, 315–321.

Barden, J. A., & Kemp, B. E. (1993) *Biochemistry 32*, 7126–7132.

Brünger, A. T., Clore, G. M., Gronenborn, A. M., & Karplus, M. (1986) *Proc. Natl. Acad. Sci. U.S.A. 83*, 3801–3805.

Bundi, A., Andreatta, R., Rittel, W., & Wüthrich, K. (1976) *FEBS Lett. 64*, 126–129.

Bundi, A., Andreatta, R. H., & Wüthrich, K. (1978) *Eur. J. Biochem. 91*, 201–208.

Caulfield, M. P., & Rosenblatt, M. (1990) *Trends Endocrinol. Metab. 1*, 164–168.

Caulfield, M. P., McKee, R. L., Goldman, M. E., Duong, L. T., Fisher, J. E., Gay, C. T., DeHaven, P. A., Levy, J. J., Roubini, E., Nutt, R. F., Chorev, M., & Rosenblatt, M. (1990) *Endocrinology 127*, 83–87.

Chiu, K. W., Lee, Y. C., & Pang, P. K. T. (1992) *Gen. Comp. Endocrinol. 86*, 506–510.

Chorev, M., Goldman, M. E., McKee, R. L., Roubini, E., Levy, J. J., Gay, C. T., Reagan, J. E., Fisher, J. E., Caporale, L. H., Golub, E. E., Caulfield, M. P., Nutt, R. F., & Rosenblatt, M. (1990) *Biochemistry 29*, 1580–1586.

Chorev, M., Roubini, E., McKee, R. L., Gibbons, S. W., Goldmann, M. E., Caulfield, M. P., & Rosenblatt, M. (1991) *Biochemistry 30*, 5968–5974.

Cohen, F. E., Strewler, G. J., Bradley, M. S., Cariquist, M., Nilsson, M., Ericsson, M., Ciardelli, T. L., & Nissenson, R. A. (1991) *J. Biol. Chem. 266*, 1997–2004.

Federau, T. (1992) Diplomarbeit (Chemie), Technical Universität, Braunschweig.

Fiskin, A. M., Cohn, D. V., & Peterson, G. S. (1977) *J. Biol. Chem. 252*, 8261–8268.

Fremlinger, A. L., & Zull J. E. (1986) *Arch. Biochem. Biophys. 244*, 641–649.

Fujimori, A., Cheng, S.-L., Avioli, L. V., & Civitelli, R. (1992) *Endocrinology 130*, 29–36.

Gardella, T. J., Axelrod, D., Rubin, D., Keutmann, H. T., Potts, J. T., Kronenberg, H. M., & Nussbaum, S. R. (1991) *J. Biol. Chem. 266*, 13141–13146.

Gardella, T. J., Wilson, A. K., Keutmann, H. T., Oberstein, R., Potts, J. T., Kronenberg, H. M., & Nussbaum, S. R. (1993) *Endocrinology 132*, 2024–2030.

Havel, T. F., & Wüthrich, K. (1984) *Bull. Math. Biol. 46*, 673–698.

Hennessey, J. P., & Johnson, W. C. (1981) *Biochemistry 20*, 1085–1094.

Ishihara, T., Nakamura, S., Kaziro, Y., Takahashi, T., Takahashi, K., & Nagata, S. (1991) *EMBO J. 10*, 1635–1641.

Jouishomme, H., Whitfield, J. F., Chakravarthy, B., Durkin, J. P., Gagnon, L., Isaacs, R. J., MacLean, S., Neugebauer, W., Willick, G., & Rixon, R. H. (1992) *Endocrinology 130*, 53–60.

Jüppner, H., Abou-Samra, A.-B., Freeman, M., Kong, X. F., Schipani, E., Richards, J., Kolakowski, L. F., Hock, J., Potts, J. T., Kronenberg, H. M., & Segre, G. V. (1991) *Science 254*, 1024–1026.

Kaiser, E. T., & Kézdy, F. J. (1987) *Annu. Rev. Biophys. Biophys. Chem. 16*, 561–581.

Klaus, W., Dieckmann, T., Wray, V., Schomburg, D., Wingender, E., & Mayer, H. (1991) *Biochemistry 30*, 6936–6942.

Lee, S. C., & Russell, A. F. (1989) *Biopolymers 28*, 1115–1127.

Lim, S. K., Gardella, T. J., Baba, H., Nussbaum, S. R., & Kronenberg, H. M. (1992) *Endocrinology 131*, 2325–2330.

Lin, H. Y., Harris, T. L., Flannery, M. S., Aruffo, A., Kaji, E. H., Gorn, A., Kolakowski, L. F., Lodish, H. F., & Goldring, S. R. (1991) *Science 254*, 1022–1024.

Murray, T. M. (1992) International Bone Forum: The First International Forum on Calcified Tissue and Bone Metabolism, Yokohama, Japan, 1992, pp 36–39.

Murray, T. M., Roa, L. G., Muzaffar, S. A., & Ly, H. (1989) *Endocrinology 124*, 1097–1099.

Neugebauer, W., Surewicz, W. K., Gordon, H. L., Somorjai, R. L., Sung, W., & Willick, G. E. (1992) *Biochemistry 31*, 2056–2063.

Niedig, K.-P., & Kalbitzer, H. R. (1990) *J. Magn. Reson. 88*, 155–160.

Nussbaum, S. R., Rosenblatt, M., & Potts, J. T. (1980) *J. Biol. Chem. 255*, 10183–10187.

Okamoto, Y., Kikuchi, T., Nakazawa, T., & Kawai, H. (1993) *Int. J. Peptide Protein Res. 42*, 300–303.

Potts, J. T. (1992) International Bone Forum: The First International Forum on Calcified Tissue and Bone Metabolism, Yokohama, Japan, 1992, pp 6–11.

Potts, J. T., Kronenberg, H. M., & Rosenblatt, M. (1982) *Adv. Protein Chem. 35*, 323–396.

Ray, F. R., Barden, J. A., & Kemp, B. E. (1993) *Eur. J. Biochem. 211*, 205–211.

Schlüter, K.-D., Hellstern, H., Wingender, E., & Mayer, H. (1989) *J. Biol. Chem. 264*, 11087–11092.

Segre, G. V., Niall, H. D., Sauer, R. T., & Potts, J. T. (1977) *Biochemistry 16*, 2417–2427.

Shah, G. V., Epand, R. M., & Orlowski, R. C. (1987) *Mol. Cell. Endocrinol. 49*, 203–210.

Sömjen, D., Binderman, I., Schlüter, K.-D., Wingender, E., Mayer, H., & Kaye, A. M. (1990) *Biochem. J. 272*, 781–785.

Sömjen, D., Schlüter, K.-D., Wingender, E., Mayer, H., & Kaye, A. M. (1991) *Biochem. J. 277*, 863–868.

Sönnichsen, F. D., Van Eyk, J. E., Hodges, R. S., & Sykes, B. D. (1992) *Biochemistry 31*, 8790–8798.

Strickland, L. A., Bozzato, R. P., & Kronis, K. A. (1993) *Biochemistry 32*, 6050–6057.

Takano, T., Takatsuki, K., Yoneda, M., Tomita, A., Ogawa, K., & Matsui, N. (1988) *Acta Endocrinol. 118*, 551–558.

Willis, K. J., & Szabo, A. G. (1992) *Biochemistry 31*, 8924–8931.

Wray, V., Kakoschke, C., Nokihara, K., & Naruse, S. (1993) *Biochemistry 32*, 5832–5841.

Wüthrich, K. (1986) *NMR of Proteins and Nucleic Acids*, Wiley, New York.

Zull, J. E., & Lev, N. B. (1980) *Proc. Natl. Acad. Sci. U.S.A. 77*, 3791–3795.

Zull, J. E., Smith, S. K., & Wiltshire R. (1990) *J. Biol. Chem. 265*, 5671–5676.